

See discussions, stats, and author profiles for this publication at: <https://www.researchgate.net/publication/262689717>

Improvement of Al₂O₃Films on Graphene Grown by Atomic Layer Deposition with Pre-H₂O Treatment

DATASET · MAY 2014

READS

56

10 AUTHORS, INCLUDING:



Xinrong Cheng

Chinese Academy of Sciences

61 PUBLICATIONS 217 CITATIONS

[SEE PROFILE](#)



Gang Wang

Lanzhou University

23 PUBLICATIONS 75 CITATIONS

[SEE PROFILE](#)



Zhongjian Wang

Chinese Academy of Sciences

32 PUBLICATIONS 49 CITATIONS

[SEE PROFILE](#)



Dawei Xu

Chinese Academy of Sciences

26 PUBLICATIONS 38 CITATIONS

[SEE PROFILE](#)

Improvement of Al_2O_3 Films on Graphene Grown by Atomic Layer Deposition with Pre- H_2O Treatment

Li Zheng,^{†,‡} Xinhong Cheng,^{*,†} Duo Cao,^{†,‡} Gang Wang,[†] Zhongjian Wang,[†] Dawei Xu,^{†,‡} Chao Xia,^{†,‡} Lingyan Shen,^{†,‡} Yuehui Yu,[†] and Dashen Shen[§]

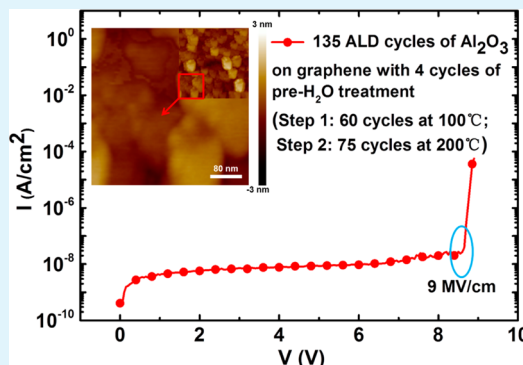
[†]State Key Laboratory of Functional Materials for Informatics, SIMIT, Chinese Academy of Sciences, Shanghai 200050, China

[‡]University of Chinese Academy of Sciences, Beijing 100049, China

[§]University of Alabama in Huntsville, Huntsville, Alabama 35899, United States

S Supporting Information

ABSTRACT: We improve the surface of graphene by atomic layer deposition (ALD) without the assistance of a transition layer or surface functionalization. By controlling gas–solid physical adsorption between water molecules and graphene through the optimization of pre- H_2O treatment and two-step temperature growth, we directly grew uniform and compact Al_2O_3 films onto graphene by ALD. Al_2O_3 films, deposited with 4-cycle pre- H_2O treatment and 100–200 °C two-step growing process, presented a relative permittivity of 7.2 and a breakdown critical electrical field of 9 MV/cm. Moreover, the deposition of Al_2O_3 did not introduce any detective defects or disorders in graphene.



KEYWORDS: graphene, pre- H_2O treatment, Al_2O_3 films, gas–solid absorption

INTRODUCTION

As a two-dimensional building block for sp^2 carbon allotropes of every other dimensionality, graphene can be stacked into three-dimensional graphite, rolled into one-dimensional nanotubes, and wrapped into zero-dimensional fullerenes. Its excellent properties such as ballistic transport and high mobility make it an ideal material for nanoelectronics.^{1–7} Furthermore, its optical absorption is only 2.3% and the Young's modulus of graphene is 1 TPa, which are ideal for micro- and nanomechanical systems, transparent and conductive electrodes, and flexible and printable optoelectronics.^{3–7} To realize graphene-based devices, high-quality dielectric films on top of graphene are required as electrostatic gate dielectrics or tunnel barriers for spin injection.^{8,9} With the purpose of effectively controlling channel carriers, dielectric layers should be as thin as a few nanometers, and of uniform coverage on graphene without any pinholes. Fortunately, ALD can satisfy these requirements. However, the surface of graphene is chemical inert and there are no dangling bonds which are necessary for surface chemical reactions during the conventional ALD processes. The existing method to overcome this challenge is functionalization of graphene surface (chemical modification, a thin oxidized metal layer, or a polymer buffer layer),^{10–15} which either increases the thickness of dielectrics or induces defects into graphene. For these reasons, several attempts were tried to grow dielectric films directly on graphene.^{15–20} For example, Rammula et al.¹⁵ reported that Al_2O_3 could be deposited directly onto graphene by O_3 -based ALD. However, graphene was partial oxidized after

this process due to strong oxidizing property of O_3 . In most conventional H_2O -based ALD processes, uniform metal oxide layers on pristine graphene is difficult to yield. Nevertheless, Dlubak et al.¹⁶ reported a large improvement in the wetting ability of ALD Al_2O_3 films by the assistance of a metallic substrate. This enhanced wetting was achieved by greatly increasing the nucleation density through the use of polar traps induced on the graphene surface by an underlying metallic substrate. Alles et al.¹⁷ used a two-step process (a HfO_2 seed layer was deposited at low temperature and the rest of the layer at high temperature) to grow HfO_2 films on graphene directly with a surface root mean square (RMS) 1.7 nm because of uneven nucleation of HfO_2 at low temperature. In our recent work,^{18–20} Al_2O_3 could be deposited directly onto graphene (mechanically transferred to SiO_2/Si substrate) by H_2O -based ALD at low growing temperature (100–130 °C), where physically absorbed water molecules on graphene contributed to Al_2O_3 growth, and Al_2O_3 was uniform with a RMS of 0.23 nm. However, the critical electric field and dielectric constant were low for loose Al_2O_3 microstructure and rich of OH^- bonds coming from low temperature growth. In this work, H_2O -based ALD technique would be further explored and optimized to obtain uniform and compact Al_2O_3 films on graphene through adjusting the ALD cycle numbers of pre- H_2O .

Received: March 21, 2014

Accepted: May 2, 2014

Published: May 2, 2014

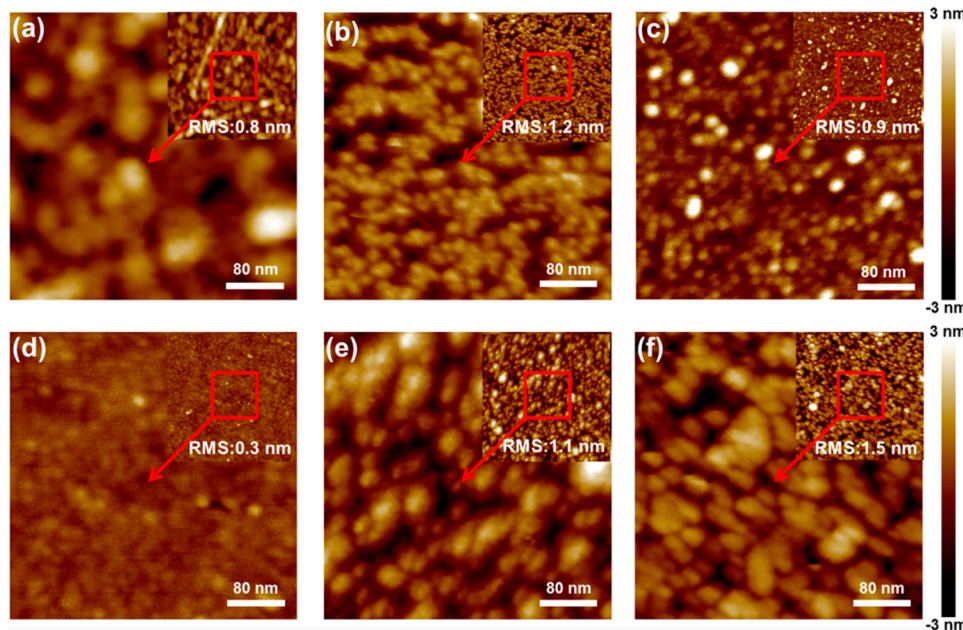


Figure 1. AFM images of Al_2O_3 films (60 ALD cycles) on graphene with different cycles of pre- H_2O treatment at 100 °C. (a) 1, (b) 2, (c) 3, (d) 4, (e) 5, and (f) 6 cycles.

treatment and regulating two-step temperature growing process. Atomic force microscope (AFM) was carried out to show how the surface morphology changed with adjusting the ALD cycle numbers of pre- H_2O treatment. Raman spectroscopy was performed to detect characteristic peaks of graphene and see whether graphene was destroyed. Transmission electron microscopy (TEM) and high-resolution TEM (HRTEM) were employed to manifest the microstructure of Al_2O_3 on graphene. X-ray photoelectron spectroscopy (XPS) was investigated to analyze the elemental compositions of Al_2O_3 films on graphene. Electrical measurements were also implemented to show the high quality of Al_2O_3 films deposited directly by ALD.

RESULTS AND DISCUSSION

Graphene surface is chemical inert and lack of dangle bonds, yet H_2O molecules can be physically absorbed onto it by van der Waals forces. Moreover, graphene is hydrophobic and difficult to be uniformly covered with H_2O molecules. This layer H_2O would act as deposition sites and its continuity will determine the morphology of Al_2O_3 seed layer. To solve this problem, we take the advantage of gas-solid physical absorption instead of liquid-solid absorption to make H_2O molecules distribute uniformly on graphene. In this process, the final H_2O molecules state is determined by three factors: the adsorption energy of H_2O molecules, the chamber temperature and the H_2O dosage. The adsorption energy is determined by the polarizability of the substrate.²¹ Theoretically, as a two-dimensional material, graphene has no polarization because of its perfect symmetry. However, the interaction of graphene with SiO_2 will induce polar traps on the graphene surface and make the carbon atom tolerate asymmetric forces from its surrounding atomics,²² leading to a residual force field, and absorb nearby H_2O molecules. The chamber temperature is correlated with the thermal energy of the H_2O molecules. At lower temperatures, due to the large dipole momentum of H_2O molecules, H_2O has a high surface affinity and is easy to form globules due to inter-molecular attraction, resulting in uneven

nucleation sites; while at higher temperatures, the thermal energy of H_2O molecules is great and excites H_2O molecules to escape from graphene surface, leading to few nucleation sites for Al_2O_3 films. In addition, The physical adsorption of H_2O molecules on graphene is similar to the process of water vapor liquefying on graphene surface and this process happens easily when the temperature of H_2O reaches to its liquefaction point (100°C).²³ Consequently, the initial ALD chamber temperature is set to 100 °C so that H_2O molecules can adhere easily to graphene by gas-solid physical absorption. Before Al_2O_3 deposition, liquid water is introduced into the ALD chamber by nitrogen and the pulse time is 10s, which is enough for water transformation between two phases (liquid and gas) and to be absorbed onto graphene. The H_2O dosage is determined by pre- H_2O treatment ALD cycle numbers. H_2O molecules act as nucleation sites and the process of pre- H_2O treatment determines the morphology of the following Al_2O_3 films, and H_2O distribution on graphene can be presented by subsequent Al_2O_3 surface morphology.

For comparison, the number of pre- H_2O treatment ALD cycles changed from 1 to 6, and the following cycle number of Al_2O_3 was fixed at 60 and the temperature was set to 100°C. The expected thickness of Al_2O_3 was 4 nm. Figures 1(a)-(f) show AFM images of Al_2O_3 films on graphene with 1-6 ALD cycles of pre- H_2O treatment, respectively. The Al_2O_3 films were not continuous and pinholes were obvious with only 1 cycle of pre- H_2O treatment, and the RMS roughness was 0.8 nm (Figure 1a). When the ALD cycles increased, Al_2O_3 films became continuous and pinholes reduced significantly (Figure 1b, c). For the sample with 4 cycles of pre- H_2O treatment, the pinholes were few and the RMS roughness was only 0.3 nm, as shown in Figure 1d, comparable to the surface of SiO_2/Si .²⁴ Continuing to increase the pre- H_2O treatment cycles to 5 or 6, the pinhole defects reappeared, as shown in images e and f in Figure 1. And the RMS roughness deteriorated to 1.1 and 1.5 nm, respectively. The poor morphology of Al_2O_3 films was due to excessive adsorption of H_2O molecules on graphene. If graphene was over treated by pre- H_2O treatment, the van der

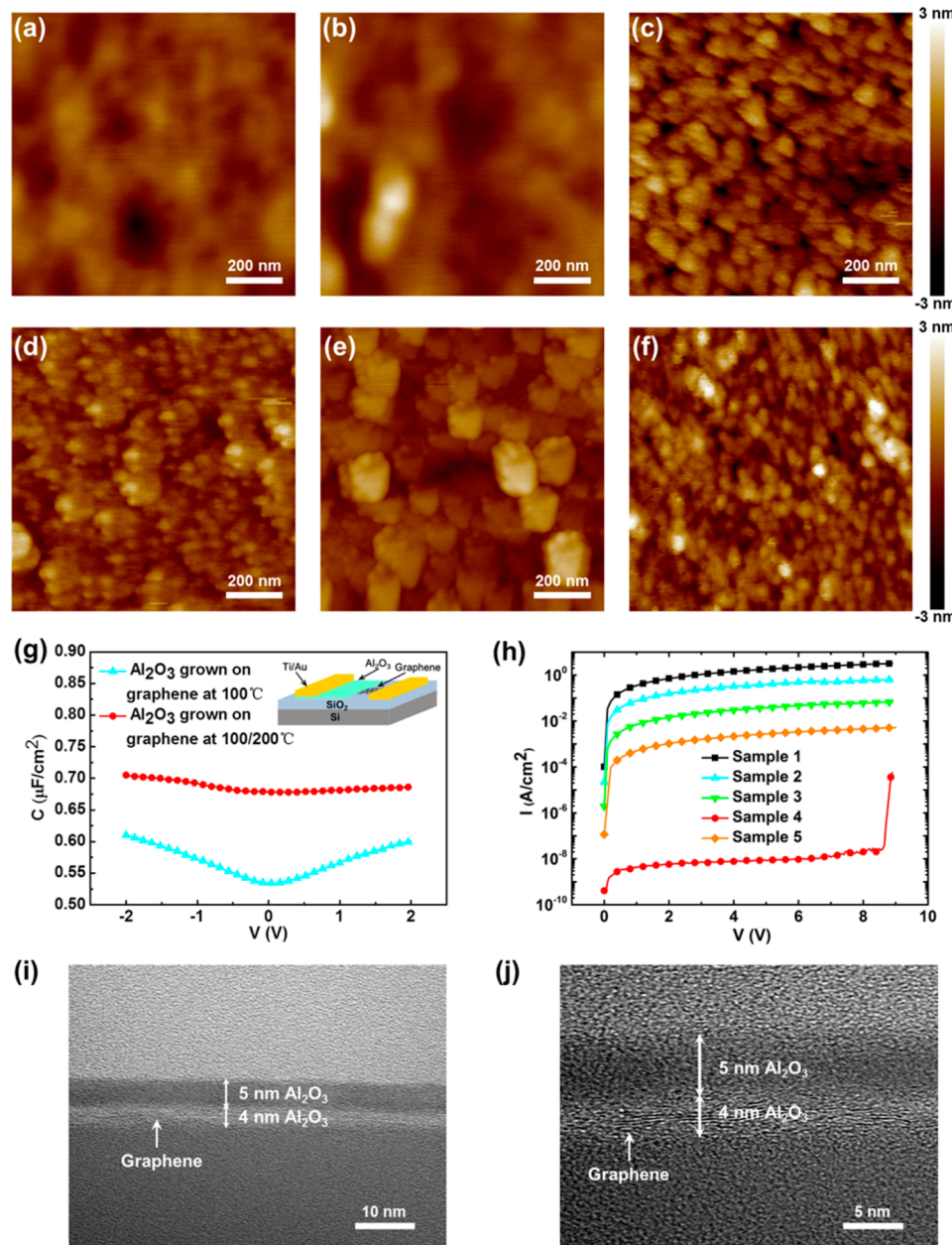


Figure 2. (a–f) AFM images of Al_2O_3 films on graphene with different assignments of ALD cycles at first-step temperature (100°C) and second-step temperature (200°C); 135 ALD cycles in total. (a) 15 cycles/120 cycles, (b) 30 cycles/105 cycles, (c) 45 cycles/90 cycles, (d) 60 cycles/75 cycles, (e) 75 cycles/60 cycles, (f) 90 cycles/45 cycles, (g) C – V measurements of 9 nm Al_2O_3 films on graphene under two different growth conditions. One was at 100°C (blue curve) and the other condition was that first 4 nm Al_2O_3 was deposited at 100°C , whereas the subsequent 5 nm Al_2O_3 was deposited at 200°C (red curve). (h) I – V_{bd} measurements of Al_2O_3 films on graphene with different assignments of ALD cycles at first-step temperature (100°C) and second-step temperature (200°C). (i) TEM image of Al_2O_3 films on graphene (sample 4). (j) HRTEM image of Al_2O_3 films on graphene (sample 4).

Waals force between H_2O molecules and graphene was not enough to overcome the inter-molecular attraction and surface tension of H_2O molecules, and H_2O molecules were not uniform on graphene, resulting in poor morphology of subsequent ALD- Al_2O_3 films. As a consequence, 4 cycles of pre- H_2O treatment is optimal for ALD- Al_2O_3 film growth on graphene.

Although the growing temperature of 100°C contributed to physical adsorption of H_2O molecules on graphene and forming uniform sites for the nucleation of Al_2O_3 films during the ALD process, Al_2O_3 was loose and the dielectric capacitance was small as $0.6 \mu\text{F}/\text{cm}^2$, shown in Figure 2g (blue curve).

Thus, to obtain compact gate dielectrics with high permittivity and critical electrical field, we tried increasing the deposition temperature. However, when the growing temperature was above 100°C , the thermal activation energy was high for H_2O molecules, and their thermal movement became strong, preventing physical absorption of H_2O molecules on graphene. Therefore, two-step temperature growth was essential to directly deposit Al_2O_3 films on graphene and the regulation of high- and low-temperature ALD cycle numbers became particular meaningful. As shown in Table 1, totally, 135 cycles of Al_2O_3 were deposited with different assignments of ALD cycles at 100 and 200°C for 5 samples. The thickness of 15

Table 1. Five Graphene Samples with Different Assignment of ALD-Al₂O₃ Cycles at 100 and 200 °C

	sample 1	sample 2	sample 3	sample 4	sample 5
ALD cycles at 100 °C	15 (~1 nm)	30 (~2 nm)	45 (~3 nm)	60 (~4 nm)	75 (~5 nm)
ALD cycles at 200 °C	120	105	90	75	60

cycles of Al₂O₃ was about 1 nm at 100 °C. For the sample with 15 first-step cycles of Al₂O₃ grown at 100 °C and 120 second-step cycles at 200 °C, the surface morphology (Figure 2b) was actually the same as pristine graphene (Figure 2a), besides a small portion covered with Al₂O₃ islands, and its leakage current was serious (Sample 1 in Figure 2h). This result was due to ALD Al₂O₃ growth mechanism. At the initial stage, the growth of Al₂O₃ was insular. With ALD cycles increasing, the Al₂O₃ islands gradually closed to their adjacent ones and formed continuous Al₂O₃ films. 15 cycles of Al₂O₃ (~1 nm) were not enough to form continuous Al₂O₃ films; moreover, when the growing temperature rose to 200 °C, the movement of H₂O molecules was aggravated and not easy to be absorbed on graphene, resulting in few deposition sites for the second-step 120 cycles ALD-Al₂O₃ growth. Elevating the number of the first-step ALD-Al₂O₃ cycles to 30 (~2 nm) at 100 °C, the Al₂O₃ coverage improved while pinholes were obvious (Figure 2c), leading to a high leakage current (Sample 2 in Figure 2h). When the first-step ALD-Al₂O₃ cycles added to 45 (~3 nm) at 100 °C, Al₂O₃ films covered the graphene surface. Nonetheless, the leakage current was still high (sample 3 in Figure 2h) because of the existing pinholes in Al₂O₃ films (Figure 2d). Continuing to increase the first-step ALD-Al₂O₃ cycles at 100 °C to 60 (~4 nm), pinholes vanished, and the Al₂O₃ films

turned impact (Figure 2e) with a very low leakage current of 1×10^{-8} A/cm² at the biases of less than 2 V (Sample 4 in Figure h). With more first-step ALD-Al₂O₃ cycles at 100 °C, (75 cycles, ~5 nm), pinholes reappeared (Figure 2f), accompanied by a relative high leakage current (Sample 5 in Figure 2h). First-step ALD cycles at 100 °C contributed to continuity of Al₂O₃ films, whereas second-step ALD cycles at 200 °C conducted to the compactness of Al₂O₃ films. If first-step ALD cycles blindly increased, the Al₂O₃ films would be loose, leading to a high leakage current. On the contrary, if first-step ALD cycles were insufficient, there would not be enough deposition sites for second-step Al₂O₃ growth, which also led to a high leakage current. Therefore, 60 ALD cycles of first-step Al₂O₃ at 100 °C were necessary and enough for subsequent second-step Al₂O₃ deposition at 200 °C. The Al₂O₃ film was compact with a capacitance of 0.7 μF/cm² as shown in Figure 2g (red curve). Its relative permittivity and the breakdown electrical field were 7.2 and 9 MV/cm, respectively, comparable with the best quality of Al₂O₃ films on Si.²⁵ The Al₂O₃ films deposited with 60 ALD cycles at 100 °C and 75 ALD cycles at 200 °C were also characterized by TEM and HRTEM. As shown in images i and j in Figure 2, the first-step Al₂O₃ films deposited at 100 °C were 4 nm and covered the graphene surface, which was beneficial to the compactness and uniformity of the second-step 5 nm Al₂O₃ films deposited at 200 °C. It is worth noting that no interfacial layer was observed after ALD Al₂O₃ growth on graphene.

The chemical compositions of Al₂O₃ films grown at two-step temperatures (60 ALD cycles at 100 °C and 75 ALD cycles at 200 °C) were characterized by XPS as shown in Figure 3a–c, proving the existence of Al₂O₃ films on graphene and analyzing the relationship between the chemical states of Al₂O₃/graphene films and their electrical performance. For comparison, Al₂O₃ films deposited on graphene at 100 °C with 135 ALD cycles was also analyzed by XPS as shown in Figure 3d–f. All the XPS peaks were calibrated with the C 1s peak position at 284.8 eV.

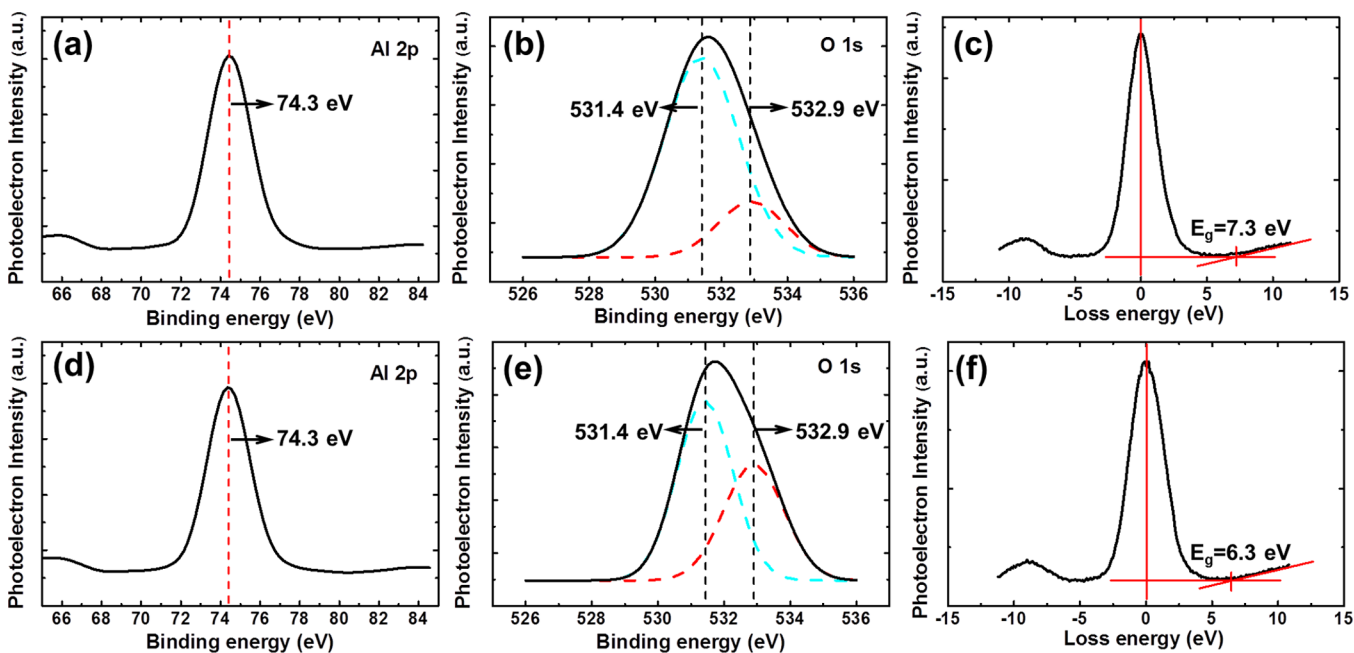


Figure 3. XPS spectra of Al₂O₃ films deposited on graphene at different temperatures. (a) Al 2p, (b) O 1s, and (c) energy-loss spectra of Al₂O₃ deposited on graphene at two-step temperatures (60 ALD cycles at 100 °C and 75 ALD cycles at 200 °C). (d) Al 2p, (e) O 1s and (f) energy-loss spectra of Al₂O₃ deposited on graphene at 100 °C (135 cycles).

For both samples, Al 2p peak could be fitted as symmetric single peaks at 74.3 eV. For the sample grown at two-step mode, O 1s peak centered at 531.7 eV and had a slight asymmetry. Further deconvolution revealed two distinct components, the stronger peak locating at 531.4 eV originated from Al–O bonds, and the other weak peak 532.9 eV associated with Al–O–H hydroxyl groups due to the incomplete reaction of TMA/H₂O at the first-step temperature (100 °C). The binding energy difference between Al 2p and O 1s was 457.4 eV, in agreement with reported values of fully oxidized amorphous Al₂O₃.^{26,27} The O/Al atomic ratio was calculated to be 1.45, close to stoichiometric Al₂O₃ of 1.5. O 1s energy-loss spectrum was also performed to calculate the band gap of Al₂O₃ on graphene (Figure 3c).^{28,29} The obtained value of 7.3 eV was close to the band gap of 8.8 eV reported for pure Al₂O₃,³⁰ and the band gap difference resulted from a few hydroxyl groups generated at the first-step temperature. For control sample, Al₂O₃ films deposited on graphene at 100 °C, the peak at 532.9 eV for O 1s spectrum became stronger than that in Figure 3b, the O/Al atomic ratio was 1.34, and the band gap reduced to 6.3 eV as shown in Figure 3f. The degraded performances for the control sample originated from the rich hydroxyl groups and defects introduced during the low-temperature (100 °C) growing process, which led to loose structure and low permittivity of Al₂O₃ films. Therefore, two-step temperatures were beneficial to Al₂O₃ structure and its electrical performance on graphene.

To understand whether H₂O-based ALD brought defects into graphene or not, we performed Raman spectroscopy to detect characteristic peaks of graphene. The Raman spectrum of monolayer graphene consists of distinct bands as shown in Figure 4, and the appearance of D and D' peaks represents the

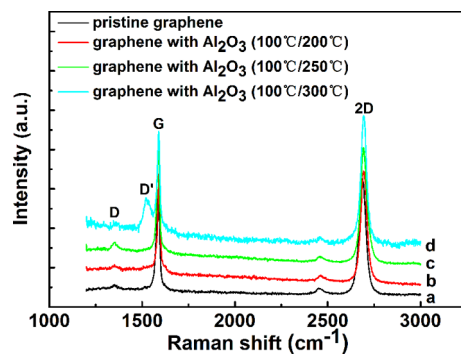


Figure 4. Raman spectra of (a) pristine graphene and (b–d) with 9 nm Al₂O₃ films deposited at different temperatures.

presence of point defects or structural disorders in graphene.^{31,32} Al₂O₃ films were deposited by two-step temperature method for three samples. 60 ALD cycles of first-step Al₂O₃ were grown at 100 °C, followed by 75 cycles of second-step Al₂O₃ grown at 200, 250, and 300 °C, respectively. When the second-step temperature regime was 200 °C, the characteristic peaks of graphene were hardly changed (Figure 4b), compared with pristine graphene (Figure 4a). Elevating the second-step temperature to 250 °C, D band heightened (Figure 4c), indicating that several defects were introduced into graphene. A significant D' peak came out (Figure 4d) when second-step temperature increased to 300 °C, giving evidence of graphene structural disruption. The high temperature of ALD chamber was responsible for defects introduction. Oxygen

diffused from Al₂O₃ to graphene interface and destroyed graphene structure when the second-step chamber temperature rose. As a result, 200 °C is a proper second-step temperature regime selection for Al₂O₃ films deposition. It is worth mentioning that Raman spectra also reveal the phenomenon of graphene G band blueshift. The blueshift of G band is due to the compressive strain in graphene developed during the ALD process,^{33,34} which indicates strong adhesion of Al₂O₃ on graphene.

CONCLUSION

In this work, we investigated a pre-H₂O treatment and two-step temperature growing ALD technique to directly deposit Al₂O₃ films on graphene, where ALD cycles of pre-H₂O treatment, two-step temperature window, and ALD cycles for certain temperature regime were optimized to control gas–solid physical adsorption. This ALD technique, introducing no detective defects or disorders into graphene, can produce uniform and compact Al₂O₃ films on graphene with a relative permittivity of 7.2 and a breakdown electrical field of 9 MV/cm. The quality of obtained Al₂O₃ films on graphene is comparable with the best quality of Al₂O₃ films on Si and it has great potential for future graphene application in microelectronics.

ASSOCIATED CONTENT

S Supporting Information

Experimental details of graphene preparation and Al₂O₃ deposition on graphene by ALD. This material is available free of charge via the Internet at <http://pubs.acs.org>.

AUTHOR INFORMATION

Corresponding Author

*E-mail: xh_cheng@mail.sim.ac.cn.

Notes

The authors declare no competing financial interest.

ACKNOWLEDGMENTS

This work was supported by the National Natural Science Foundation of China (Grant 11175229). We thank Prof. Zengfeng Di, Dr. Xiaohu Zheng, and Dr. Haoran Zhang for their generous help.

REFERENCES

- (1) Li, D.; Kaner, R. B. Graphene-Based Materials. *Science* **2008**, *320*, 1170–1171.
- (2) Rao, C. N. R.; Sood, A. K.; Subrahmanyam, K. S.; Govindaraj, A. Graphene: The New Two-Dimensional Nanomaterial. *Angew. Chem. Int. Ed.* **2009**, *48*, 7752–7777.
- (3) Geim, A. K.; Novoselov, K. S. The Rise of Graphene. *Nat. Mater.* **2007**, *6*, 183–191.
- (4) Katsnelson, M. I. Graphene: Carbon in Two Dimensions. *Mater. Today* **2007**, *10*, 20–27.
- (5) Rao, C. N. R.; Biswas, K.; Subrahmanyam, K. S.; Govindaraj, A. Graphene, The New Nanocarbon. *J. Mater. Chem.* **2009**, *19*, 2457–2469.
- (6) Singh, V.; Joung, D.; Zhai, L.; Das, S.; Khondaker, S. I.; Seal, S. Graphene Based Materials: Past, Present and Future. *Prog. Mater. Sci.* **2011**, *56*, 1178–1271.
- (7) Novoselov, K. S.; Fal'ko, V. I.; Colombo, L.; Gellert, P. R.; Schwab, M. G.; Kim, K. A Roadmap for Graphene. *Nature* **2012**, *490*, 192–200.
- (8) Chae, S. H.; Yu, W. J.; Bae, J. J.; Duong, D. L.; Perello, D.; Jeong, H. Y.; Ta, Q. H.; Ly, T. H.; Vu, Q. A.; Yun, M.; Duan, X.; Lee, Y. H. Transferred Wrinkled Al₂O₃ for Highly Stretchable and Transparent

- Graphene–carbon Nanotube Transistors. *Nat. Mater.* **2013**, *12*, 403–409.
- (9) Liao, L.; Bai, J.; Lin, Y.; Qu, Y.; Huang, Y.; Duan, X. High Performance Top-Gated Graphene Nanoribbon Transistors Using Zirconium Oxide Nanowires as High-k Gate Dielectrics. *Adv. Mater.* **2010**, *22*, 1941–1945.
- (10) Lee, B.; Mordi, G.; Kim, M. J.; Chabal, Y. J.; Vogel, E. M.; Wallace, R. M.; Cho, K. J.; Colombo, L.; Kim, J. Characteristics of High-k Al_2O_3 Dielectric Using Ozone-based Atomic Layer Deposition for Dual-gated Graphene Devices. *Appl. Phys. Lett.* **2010**, *97*, 043107.
- (11) Hollander, M. J.; LaBella, M.; Hughes, Z. R.; Zhu, M.; Trumbull, K. A.; Cavalero, R.; Snyder, D. W.; Wang, X.; Hwang, E.; Datta, S.; Robinson, J. A. Enhanced Transport and Transistor Performance with Oxide Seeded High- κ Gate Dielectrics on Wafer-scale Epitaxial Graphene. *Nano Lett.* **2011**, *11*, 3601–3607.
- (12) Fallahazad, B.; Lian, K. G.; Kim, S.; Corbet, C. M.; Ferrer, D. A.; Colombo, L.; Tutuc, E. Scaling of Al_2O_3 Dielectric for Graphene Field-effect Transistors. *Appl. Phys. Lett.* **2012**, *100*, 093112.
- (13) Tinchev, S. S. Surface Modification of Diamond-like Carbon Films to Graphene under Low Energy Ion Beam Irradiation. *Appl. Surf. Sci.* **2012**, *258*, 2931–2934.
- (14) Liu, L.; Xie, D.; Wu, M.; Yang, X.; Xu, Z.; Wang, W.; Bai, X.; Wang, E. Controlled Oxidative Functionalization of Monolayer Graphene by Water-vapor Plasma Etching. *Carbon* **2012**, *50*, 3039–3044.
- (15) Rammula, R.; Aarik, L.; Kasikov, A.; Kozlova, J.; Kahro, T.; Matisen, L.; Niilisk, A.; Alles, H.; Aarik, J. Atomic Layer Deposition of Aluminum Oxide Films on Graphene. *IOP Conf. Ser. : Mater. Sci. Eng.* **2013**, *49*, 012014.
- (16) Dlubak, B.; Kidambi, P. R.; Weatherup, R. S.; Hofmann, S.; Robertson, J. Substrate-assisted Nucleation of Ultra-thin Dielectric Layers on Graphene by Atomic Layer Deposition. *Appl. Phys. Lett.* **2012**, *100*, 173113.
- (17) Alles, H.; Aarik, J.; Aidla, A.; Fay, A.; Kozlova, J.; Niilisk, A.; Pärä, M.; Rähn, M.; Wiesner, M.; Hakonen, P.; Sammelselg, V. Atomic Layer Deposition of HfO_2 on Graphene from HfCl_4 and H_2O . *Cent. Eur. J. Phys.* **2011**, *9*, 319–324.
- (18) Zhang, Y.; Wan, L.; Cheng, X.; Wang, Z.; Xia, C.; Cao, D.; Jia, T.; Yu, Y. Studies on H_2O -Based Atomic Layer Deposition of Al_2O_3 Dielectric on Pristine Graphene. *J. Inorg. Mater.* **2012**, *27*, 956–960.
- (19) Zhang, Y.; Qiu, Z.; Cheng, X.; Xie, H.; Wang, H.; Xie, X.; Yu, Y.; Liu, R. Direct Growth of High-quality Al_2O_3 Dielectric on Graphene Layers by Low-temperature H_2O -based ALD. *J. Phys. D: Appl. Phys.* **2014**, *47*, 055106.
- (20) Zheng, L.; Cheng, X.; Cao, D.; Wang, Z.; Xia, C.; Yu, Y.; Shen, D. Property Transformation of Graphene with Al_2O_3 Films Deposited Directly by Atomic Layer Deposition. *Appl. Phys. Lett.* **2014**, *104*, 023112.
- (21) Liu, H.; Xu, K.; Zhang, X.; Ye, P. D. The Integration of High-k Dielectric on Two Dimensional Crystals by Atomic Layer Deposition. *Appl. Phys. Lett.* **2012**, *100*, 152115.
- (22) Shin, Y. J.; Wang, Y.; Huang, H.; Kalon, G.; Wee, A. T. S.; Shen, Z.; Bhatia, C. S.; Yang, H. Seeding Atomic Layer Deposition of High-k Dielectric on Graphene with Ultrathin Poly(4-vinylphenol) Layer for Enhanced Device Performance and Reliability. *Langmuir* **2010**, *26*, 3798–3802.
- (23) Qu, J. *Physical Chemistry*; China Renmin University Press: Beijing, China, 2009.
- (24) Deshpandea, A.; LeRoy, B. Scanning Probe Microscopy of Graphene. *Phys. E* **2012**, *44*, 743–759.
- (25) Groner, M. D.; Elam, J. W.; Fabreguette, F. H.; George, S. M. Electrical Characterization of Thin Al_2O_3 Films Grown by Atomic Layer Deposition on Silicon and Various Metal Substrates. *Thin Solid Films* **2002**, *413*, 186–197.
- (26) Renault, O.; Gosset, L. G.; Rouchon, D.; Ermolieff, A. Angle-resolved X-ray Photoelectron Spectroscopy of Ultrathin Al_2O_3 Films Grown by Atomic Layer Deposition. *J. Vac. Sci. Technol. A* **2002**, *20*, 1867–1876.
- (27) van den Brand, J.; Snijders, P. C.; Sloof, W. G.; Terry, H.; deWit, J. H. W. Acid-base Characterization of Aluminum Oxide Surfaces with XPS. *J. Phys. Chem. B* **2004**, *108*, 6017–6024.
- (28) Chen, X.; Liu, L.; Yu, P. Y.; Mao, S. S. Increasing Solar Absorption for Photocatalysis with Black Hydrogenated Titanium Dioxide Nanocrystals. *Science* **2011**, *331*, 746–750.
- (29) Miyazaki, S. Photoemission Study of Energy-band Alignments and Gap-state Density Distributions for High-k Gate Dielectrics. *J. Vac. Sci. Technol. B* **2001**, *19*, 2212–2216.
- (30) French, R. H. Electronic Band Structure of Al_2O_3 with Comparison to AlON and AlN. *J. Am. Ceram. Soc.* **1990**, *73*, 477–489.
- (31) Ferrari, A. C.; Meyer, J. C.; Scardaci, V.; Casiraghi, C.; Lazzeri, M.; Mauri, F.; Piscanec, S.; Jiang, D.; Novoselov, K. S.; Roth, S.; Geim, A. K. Raman Spectrum of Graphene and Graphene Layers. *Phys. Rev. Lett.* **2006**, *97*, 187401.
- (32) Ferrari, A. C.; Basko, D. M. Raman Spectroscopy as A Versatile Tool for Studying The Properties of Graphene. *Nat. Nanotechnol.* **2013**, *8*, 235–246.
- (33) Mohiuddin, T. M. G.; Lombardo, A.; Nair, R. R.; Bonetti, A.; Savini, G.; Jalil, R.; Bonini, N.; Basko, D. M.; Galiotis, C.; Marzari, N.; Novoselov, K. S.; Geim, A. K.; Ferrari, A. C. Uniaxial Strain in Graphene by Raman Spectroscopy: G Peak Splitting, Grüneisen Parameters, and Sample Orientation. *Phys. Rev. B* **2009**, *79*, 205433.
- (34) Robinson, J. A.; LaBella, M.; Trumbull, K. A.; Weng, X.; Cavalero, R.; Daniels, T.; Hughes, Z.; Hollander, M.; Fanton, M.; Snyder, D. Epitaxial Graphene Materials Integration: Effects of Dielectric Overlays on Structural and Electronic Properties. *ACS Nano* **2010**, *4*, 2667–2672.